The Use of Area Covered by Blood Vessels in Fundus Images to Detect Glaucoma

Afolabi Oluwatobi J. , Gugulethu Mabuza-Hocquet [2,] and Fulufhelo V. Nelwamondo[3]

[1] University of Johannesburg, Johannesburg, South Africa.
afolabij@uj.ac.za

[2] Council for Scientific and Industrial Research, Pretoria, South Africa.
gmabuza@csir.co.za

[3] Council for Scientific and Industrial Research, Pretoria, South Africa.
fnelwamondo@csir.co.za

Abstract. Several techniques have been employed to detect glaucoma from optic discs. Some techniques involve the use of the optic cup-to-disc ratio (CDR) while others use the neuro-retinal rim width of the optic disc. In this work, we use the area occupied by segmented blood vessels from fundus images to detect glaucoma. Blood vessels segmentation is done using an improved U-net Convolutional Neural Network (CNN). The area occupied by the blood vessels is then extracted and used to diagnose glaucoma. The technique is tested on the DR-HAGIS database and the HRF database. We compare our result with a similar method called the ISNT-ratio which involves the use of the Inferior, Superior, Nasal and Temporal neuro- retina rims. The ISNT-ratio is expressed as the ratio of the sum of blood vessels in the Inferior and the Superior to the sum of blood vessels in the Nasal and Temporal. Our results demonstrate a more reliable, stable and efficient method of detecting glaucoma from segmented blood vessels. Our results also show that segmented blood vessels from healthy fundus images cover more area than those from glaucomatous and diabetic fundus images.

Keywords: Retinal Fundus Image, Glaucoma, Blood Vessel Segmentation, Image segmentation.

1 Introduction

Glaucoma is an eye diseases which is marked by gradual and continuous loss of the optic disc as well as the retinal ganglion cells [1, 2]. Second only to diabetic retinopathy, glaucoma is a leading cause of blindness. Hence, it's early detection and treatment is of great importance.

A common technique for the detection of glaucoma is the determination of the Cup-to –disc ratio (CDR) from the fundus image as seen in Fig.1. Alternative to using CDR technique is the use of the neuro-retina rim width of the optic disc. The neuro-retinal rim width is the measured length or thickness between the boundary of the optic cup and the optic disc [3-5]. The width measurement is taken for four different regions of

the optic disc. The four regions are obtained by dividing the optic disc into quadrants as shown in Fig. 2. The quadrants are (i) The lower quadrant region known as the Inferior, (ii) The upper quadrant region known as the Superior, (iii) The left quadrant region known as the Nasal and (iv) The right quadrant region known as the Temporal [6-12].
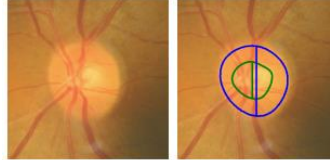

Fig. 1. Determination of cup-to-disc ratio. The inner circle is the segmented cup and the outer circle is the segmented disc [13]

Few methods have been used to detect glaucoma from segmented blood vessels. One of such methods is the ISNT-ratio. This is the ratio of the sum of blood vessels in the Superior and Inferior to the sum of blood vessels in the Nasal and Temporal i.e:

$$(I + S) / (N + T) \tag{1}$$

Where I is the area of inferior blood vessel quadrant, S is area of superior blood vessel quadrant, N is area of nasal blood vessel quadrant and T is the area of temporal blood vessel quadrant. However, this method is unstable and the optimum value of ISNT-ratio to use as discriminant between glaucomatous and non-glaucomatous fundus images varies across database and across authors reviewed. Hence, the method is very subjective.

In this work, we propose a method that detects glaucoma from fundus images based on the area covered by segmented blood vessels. The segmentation process is done using an improved U-net Convolutional Neural Network (CNN). A CNN [14] is used because of its adaptable and less context specific nature i.e. it generalizes well on unseen fundus images [15-17]. The modified U-net architecture used in this work has much less number of parameters than the traditional U-net [18].

This work uses the HRF [18, 20] and the DR HAGIS databases [21]. The databases consist of labelled fundus images as well as their corresponding segmented blood vessels. Both the proposed method and the ISNT-ratio method are evaluated on the databases. The ability of our proposed method to separate glaucomatous fundus from non-glaucomatous fundus images is measured against that of the ISNT-ratio technique.

The contribution made by this work include a method of glaucoma detection that makes use of area covered by blood vessels in fundus images. Also, a result analysis of both the proposed and the ISNT-ratio methods is provided.

The rest of this paper is organized as follows: section 2 discusses the related work, section 3 discusses the proposed approach of the experiment, section 4 presents the results of the experiment and section 5 discusses the limitations of the study. Section 6 presents the conclusion and the last section explains the future work.

2   Related Work

The detection of glaucoma from fundus images involves two major processes which are; segmentation of blood vessels from fundus images and extraction of desired features from the segmented blood vessels. This section discusses the various segmentation methods that have been used and the subsequent use of segmented blood vessels for glaucoma detection.

Segmentation processes are usually carried out using CNNs because of their robust and efficient result. Pre-trained CNN model was used by Sunil *et al.* [22] for blood vessels segmentation. The model used was pre-trained on the Microsoft COCO dataset [23]. Training of the model was done using patches from the fundus images. Hence, the outputs of the model are segmented image patches which were recombined to form the desired segmented blood vessels. Sonro *et al.* [24] used a method that involves both a pre-processing of the fundus images and a post pro-processing of the output. Pre-processing includes ensuring uniform illumination of fundus, conversion of fundus images to a grey scale and rescaling of the images. The post-processing includes the application of a double threshold on the output. The model used was a CNN. Oliveira *et al.* [25] employed the combination of stationary wavelet transformations and a fully CNN. The transformations were done on the fundus images before they were fed into the CNN in patches. The above discussed methods of blood vessel segmentation involve a lot of pre- processing and post-processing. These processes make the methods to be cumbersome.

After a proper segmentation process, some analysis must be carried out in order to detect which ocular disease is present. One of the analysis needed to detect which ocular disease is present is based on a variant of the ISNT rule. For segmented fundus images, the ratio of the number of blood vessels in the neuro-retina rims is often used as a feature to detect glaucomatous eye.

Shyam et al. [26] proposed a glaucoma detection technique that makes use of segmented blood vessels from the fundus image. The analysis of the blood vessel is done using the ISNT-ratio. The ISNT-ratio used is computed as shown in (1). The analysis is performed on 10 glaucomatous and 10 non-glaucomatous fundus images. The ISNT ratio is calculated for all of the segmented fundus images. Their work reports that ISNT ratio of non-glaucomatous fundus images is higher than that of glaucomatous fundus images. This is because more blood vessels are lost in a glaucomatous fundus as a result of increased pressure in the eye. They concluded that the ISNT ratio for a non-glaucomatous fundus image is within the range of 2.166 ± 0.19 and 1.755 ± 0.08 for a glaucomatous fundus image. The difference in range allows for separation of healthy eyes from glaucomatous eyes. Jeyashree *et al.* [6] also detected glaucoma from segmented blood vessels using the ISNT-ratio as shown in (1). They did this by using a mask image of 360x360 to evaluate the area occupied by blood vessels in each of the ISNT quadrant. Their report shows that the average number of blood vessels in a non-glaucomatous fundus image is 29254.3 ± 10775.5 and 35746 ± 11443.2 in a glaucomatous fundus image. Their report also shows that the average ISNT ratio for non-glaucomatous and glaucomatous fundus image are 1.024 ± 0.02 and 1.037 ± 0.021 respectively.

However, *Jeyashree et al.* concluded that the number of blood vessels are higher in non-glaucomatous fundus images than in glaucomatous images. Deepika *et al.* [27] also proposed a glaucoma detection technique using blood vessel segmentation. However, they did not use the ISNT-ratio for blood vessel classification into glaucoma or non-glaucoma but rather used statistical features extracted from blood vessels. The statistical feature used were entropy, mean and standard deviation. Deepika *et al.* reported that the average entropy, mean and standard deviation for healthy fundus images are 7.0591, 87.279 and 77.049 respectively. For a glaucomatous fundus image, they are 5.6832, 54.121 and 58.086 respectively. They proposed that the entropy, mean and standard deviation are higher in non-glaucoma fundus images.

It should be noted that the ISNT-ratio range quoted by Jeyashree *et al.* is very different from those quoted by Shyam *et al.* [26] for both non-glaucomatous and glaucomatous fundus images. This suggests that the ISNT- ratio is dependent on the source of the fundus image and the image processing technique used. A glaucoma detection method which is independent of the source of database used and the image processing technique adopted is therefore needed.

3   Proposed Experimental Approach

The Blood vessel segmentation from the fundus images is done using a CNN architecture based on the U-net. When compared to the original U-net, the proposed architecture as shown in Fig.2 has more convolutional layers. Though the proposed CNN architecture has more layers, the filter size (3x3) is kept the same in all layers except the output layer which has a filter size of 1x1. The proposed architecture has much less number of parameters than the earliest U-Net. Our experiment revealed that networks with large parameters over-fit quickly on the training data and therefore generalizes poorly for segmentation tasks. The U-net architecture was set up as described in Afolabi *et al.* [28].

The fundus images are scaled down to 512x512 pixels so as to reduce computation time and cost. The re-scaling has no negative impact on the training process, it rather increases the training speed. The contrast of the fundus images is further enhanced using the histograms calculated over several tile regions of the image. Scikit equalize adapthist is used for this process. Improving the contrast makes the fundus images to have uniform contrast and hence, better training of model. The improved contrast fundus images are fed into the CNN model.
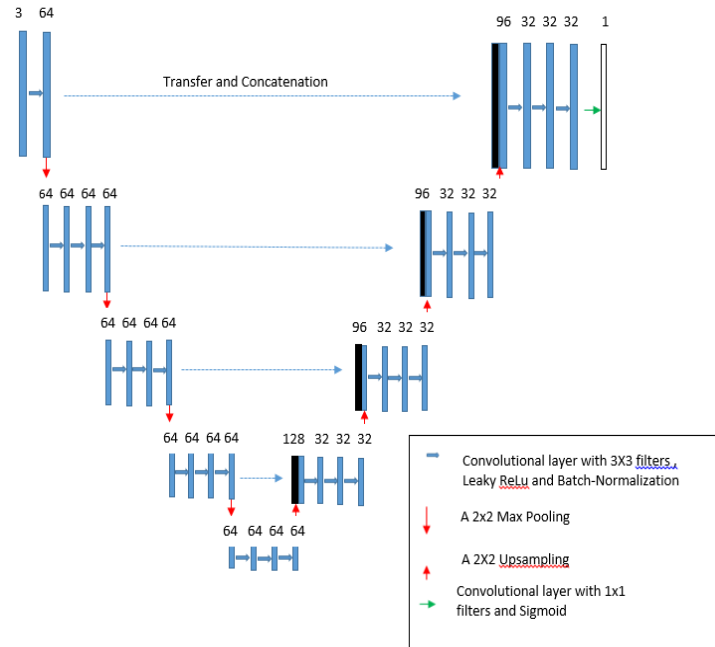
Fig. 2. Proposed model architecture for extraction of blood vessels from fundus images

The segmented and re-sized fundus images are then processed to obtain the area occupied by the blood vessels. This is done by binarizing the images and extracting active pixels. The extracted area is normalized to remove the effect of varying image- size across different databases. To obtain the ISNT-ratio of the fundus images, we mask the segmented and resized fundus images along their sectors to obtain the Inferior (I), Superior (S), Nasal (N) and Temporal (T) quadrants as shown in Fig. 3. This is done using the ogrid library of the numpy package. The number of blood vessels in each quadrant is then obtained. The obtained number of vessels is used to compute the ISNT ratio. The ISNT ratio is the ratio of the addition of area covered by the Inferior and Superior quadrants to the addition of the area covered by the Nasal and Temporal quadrants.
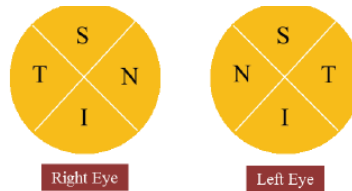

Fig. 3. Optic disc divided into the ISNT quadrants. For the right and Left eye respectively [29]

The proposed approach is further described by the following algorithm.

Step 1: Re-sizing the images to 512 x 512 pixels

Step 2: Applying histogram equalization to images

Step 3: Training the modified U-net CNN with the re-sized fundus images.

The output of step 3 are segmented blood vessels from fundus images. Fig. 4 explains the further processes applied to the segmented images.
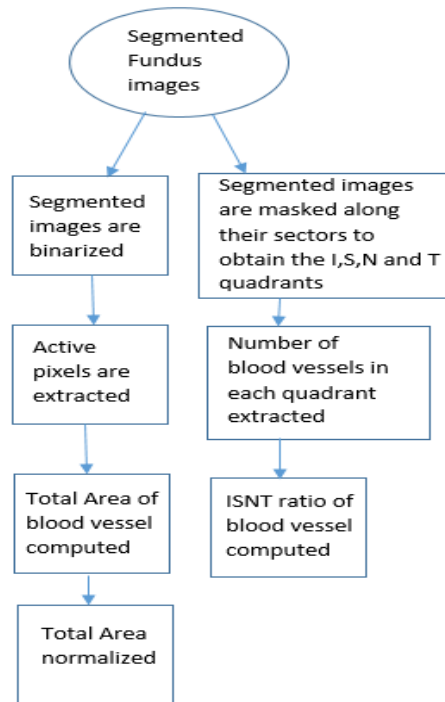

Fig. 4. Proposed flow chart for Total area and ISNT ratio acquisition

Figure 5 shows a fundus image and a segmented fundus image from which the total area of blood vessel is acquired.
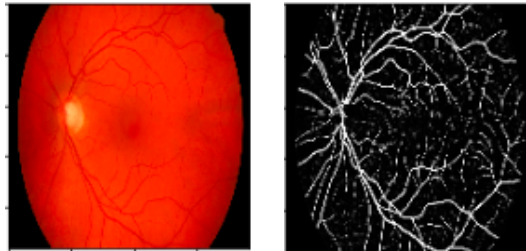

Fig. 5. Fundus image (Left), Segmented Fundus image (R)

Figure 6 shows the I, S, N and T quadrants from which the ISNT-ratio values are obtained
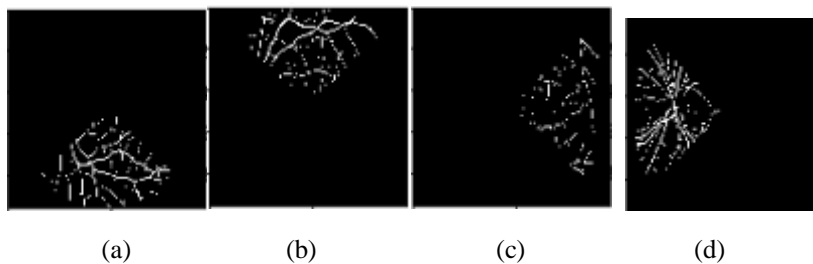

(a)   (b)   (c)   (d)

Fig. 6. Fundus images for the extraction of ISNT-ratio values. (a) I quadrant (b) S quadrant (c) N quadrant (d) T quadrant

4 Experimental Results

The experiment is tested on fundus images from HRF and DR-HAGIS database. The HRF database has 45 images of size 3504 x 2336 and the DR-HAGIS database has 40 images of varying size from 4752x3168 to 2896 x 1944. The DR-HAGIS database has images from glaucoma, hypertension, diabetic retinopathy and age-related macular diseases. The experiment was carried out using Kaggle's 2 CPU cores, 14 GB RAM.

We compare our proposed method's results for the glaucomatous with the non-glaucomatous segmented fundus images. The comparison was done to see the differences in the area occupied by glaucomatous and the non-glaucomatous fundus images. The differences becomes the bases for separation between non-glaucomatous and glaucomatous segmented fundus image. The same process was repeated for the ISNT-ratio method. Some results are shown in Table I and Table 2 for the HRF and DR-HAGIS database respectively.

Table 1. Area Covered by segmented blood vessels and ISNT-ratio values for the HRF database

Area Covered by Non-glaucomatous Fundus (/pixels)	Area Covered by glaucomatous Fundus (/pixels)	ISNT ratio For Non-glaucomatous Fundus	ISNT ratio For Glaucomatous Fundus
0.081	0.063	1.134	1.315
0.093	0.069	1.263	1.069
0.091	0.072	1.165	1.247
0.087	0.062	1.074	1.135
0.082	0.066	1.169	1.219

Table 1 shows some of the 45 segmented fundus images' ISNT-ratio and area covered by blood vessels for the HRF database. The samples displayed in Table 1 are randomly picked from the entire samples. It can be seen that the area (per pixel) occupied by non-glaucomatous images are higher than that of the glaucomatous images. This is because non-glaucomatous images have healthier blood vessels while glaucomatous images are often marked with gradual loss of blood vessels. The ISNT-ratio values for both glaucomatous and non-glaucomatous fundus images are inter-twined as observed from Table 1. This makes differentiating between non-glaucomatous and glaucomatous fundus images impossible in most cases.

Table 2. Area Covered by Fundus images and ISNT-ratio values for the DR-HAGIS database

Area Covered by glaucomatous Fundus (/pixels)	ISNT ratio For Glaucomatous Fundus
0.0523	1.2654
0.0567	1.760
0.069	1.629
0.053	1.545
0.048	1.917

Table 2 shows some of the 40 segmented fundus images' ISNT-ratio and area covered by blood vessels for the DR-HAGIS database. The DR-HAGIS database does not have non-glaucomatous fundus images. The database was selected to compare the area covered by glaucomatous fundus images and some other ocular diseases with that of non-glaucomatous fundus images of another database. This assures that the values are consistent or at least close across different databases. The table shows that the area covered by glaucomatous fundus images is comparable with that of the HRF database and it is below the range of the non-glaucomatous images.

Figure 7 shows the scatter plot of the area covered by blood vessels in each fundus image of the HRF-database. It can be seen that fundus images with higher area per pixel are non-glaucomatous fundus images. This helps to set a boundary that guarantees that a fundus image is non-glaucomatous. The boundary is drawn in Fig. 9.

Figure 8 shows the scatter plot of the ISNT-ratio value for each fundus image in the HRF-database. From the figure, there is no clear boundary between the glaucomatous and the non-glaucomatous fundus images. This makes using the method as a means of differentiating between the glaucomatous and non-glaucomatous fundus images inefficient.

Figure 9 shows the scatterplot of the area covered by blood vessels in each fundus image of the DR-HAGIS database interpolated on those of the HRF database. This helps to give a clear view of the method's performance across two different database.

From the figure, it can be seen that there is a demarcation between glaucomatous and non-glaucomatous fundus images. An area of 0.08 per pixel is a good value to pick as a boundary. In other words, a fundus image with an area occupied by blood vessel of 0.08 per pixel or above is non-glaucomatous.
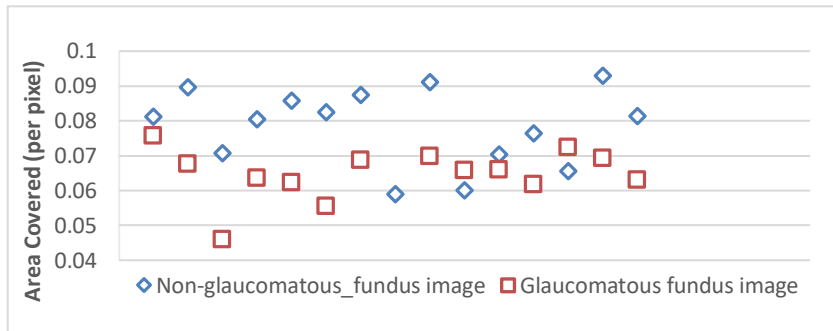

Fig. 7. Area covered by segmented blood vessels in each fundus image of the HRF database.
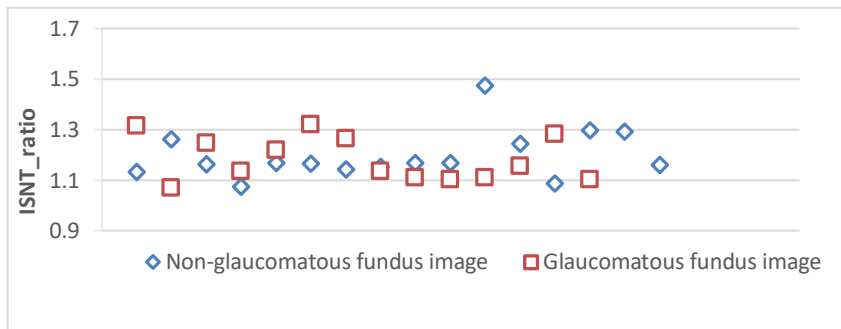

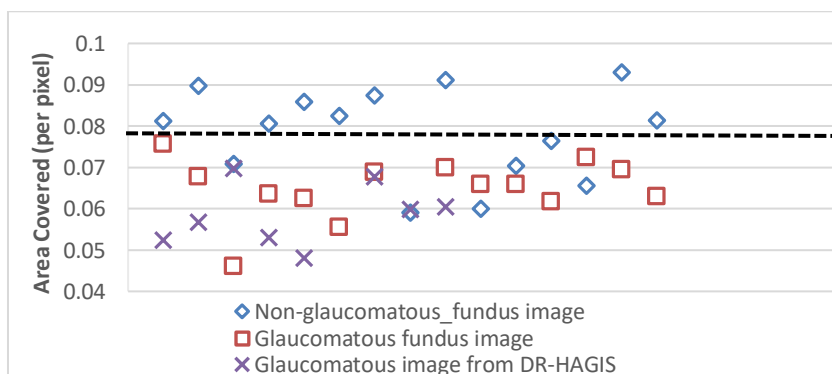**Fig. 8.** ISNT-ratio of each fundus image in the HRF database

Fig. 9. Area covered by segmented blood vessels in fundus images from the HRF database overlaid by glaucomatous images from the DR-HAGIS database

5   Limitation of the Study

The study is affected by some anomalies in the database used. This is because fundus images marked non-glaucomatous could also be affected by other ocular disease not captured by the database. Also, the accuracy of the method proposed depends on the goodness of the segmentation process used on the fundus images.

6   Conclusion

The proposed method performed better on the two databases when compared with the ISNT-ratio method. The proposed method is especially useful when used to detect non-glaucomatous fundus images since non-glaucomatous fundus images have higher area-value. However, for optimum result, the proposed method should not be used alone for the detection of glaucoma in fundus images. It should be used in conjunction with other techniques of glaucoma detection such as the CDR.

7   Future Work

The same procedure will be carried out using more databases. The use of more databases will give a more generalized value to be used as a boundary of separation. Also, the performance of this method will also be evaluated against other methods of glaucoma detection.

References

1.   Qiu K, Wang G, Lu X, Zhang R, Sun L and Zhang M.: Application of the ISNT rules on retinal nerve fibre layer thickness and neuroretinal rim area in healthy myopic eyes. Acta Ophthalmologica. DOI: 10.1111/aos.13586 (2018).
2.   Moon J, Park KH, Kim DM and Kim SH.: Factors Affecting ISNT Rule Satisfaction in Normal and Glaucomatous Eyes.Korean journal of ophthalmology. KJO. DOI: 10.3341/kjo.2017.0031 (2018).
3.   Ahmad H, Yamin A, Shakeel A, Gillani SO and Ansari U.: Detection of glaucoma using retinal fundus images. In: IEEE, International Conference on Robotics and Emerging Allied Technologies in Engineering 2014, pp.321-324 (2014).
4.   Bhartiya S, Gadia R, Sethi H.S. and Panda A.: Clinical evaluation of optic nerve head in glaucoma. Current Journal of Glaucoma Practice with DVD, 4:115{132}, doi:10.5005/jp-journals-10008-1080 (2010)
5.   Das P., Nirmala S.R., Medhi J.P.: Detection of glaucoma using neuroretinal rim information, in International Conference on Accessibility to Digital World (ICADW) 2016, pp. 181-186 (2016).

6. Jeyashree D., .Ramasamy K.: Combined Approach on Analysis of Retinal Blood Vessel Segmentation for Diabetic Retinopathy and Glaucoma Diagnosis. vol. 5, 2014.

7. G. R. Foundation. Five common glaucoma tests. URL https://www.glaucoma.org/glaucoma/diagnostic-tests.php.9 last accessed 2019/09/13

8. Moon J., Park K.H., Kim D.M., Kim S.H.: Factors Affecting ISNT Rule Satisfaction in Normal and Glaucomatous Eyes. Korean Journal of Ophthalmology: KJO, vol. 32, *(1),* pp. 38-44 (2018).

9. Shyam L. and Kumar G.S.: Blood vessel segmentation in fundus images and detection of glaucoma. In: International Conference on Communication Systems and Networks (ComNet) 2016, pp. 34-38 (2016).

10. Kang D. and Sowka J.: The ISNT rule is a clinically useful method to aid in the diagnosis of glaucoma. Optometry - Journal of the American Optometric Association, vol. 82, (3), pp. 134, 2011.

11. Poon L.Y., Solá-Del Valle D., Turalba A. V., Falkenstein I. A., Horsley M., Kim J. H., Song B. J., Takusagawa H. L.,Wang K. and Chen T. C.: The ISNT Rule: How Often Does It Apply to Disc Photographs and Retinal Nerve Fiber Layer Measurements in the Normal Population?. American Journal of Ophthalmology, vol. 184, pp. 19-27 (2017).

12. Nawaldgi F. and Lalitha Y.S.: A Novel Combined Color Channel and ISNT Rule Based Automatic Glaucoma Detection from Color Fundus Images. Indian Journal of Science and Technology, vol. 10, *(13),* pp. 1-6, (2017).

13. Lim G., Cheng Y., Hsu W., and Lee M.L.; Integrated optic disc and cup segmentation with deep learning. pages 162{169. IEEE, Nov 2015. ISBN 1082-3409. doi: 10.1109/ICTAI.2015.36. URL https://ieeexplore.ieee.org/document/7372132 (2015).

14. Shelhamer E., Long J. and Darrell T.; Fully Convolutional Networks for Semantic Segmentation. Tpami, vol. 39, (4), pp. 640-651 (2017).

15. Sunil Kumar Vengalil, Neelam Sinha, Srinivas S S Kruthiventi and R Venkatesh Babu.: Customizing CNNs for blood vessel segmentation from fundus images. In: The Institute of Electrical and Electronics Engineers, Inc. (IEEE) Conference Proceedings 2016, pp. 1. (2016).

16. Soomro T. A., Afifi A. J., Junbin G., Hellwich O., Khan M. A., Paul M. and Lihong Zheng.: Boosting sensitivity of a retinal vessel segmentation algorithm with convolutional neural network. In: International Conference on Digital Image Computing: Techniques and Applications 2017, DICTA, pp. 1-8. (2017)

17. A. Oliveira, S. Pereira and C. A. Silva, "Retinal vessel segmentation based on Fully Convolutional Neural Networks," Expert Systems with Applications, vol. 112, pp. 229-242, 2018. Available: https://www.sciencedirect.com/science/article/pii/S0957417418303816. DOI: 10.1016/j.eswa.2018.06.034.

18. O. Ronneberger, P. Fischer and T. Brox, "U-Net: Convolutional Networks for Biomedical Image Segmentation," 2015. Available: http://arxiv.org/abs/1505.04597.

19. A. Budai, R. Bock, A. Maier, J. Hornegger and G. Michelson, "Robust Vessel Segmentation in Fundus Images," *International Journal of Biomedical Imaging,* vol. 2013, pp. 154860-11, 2013. Available: http://dx.doi.org/10.1155/2013/154860.

20. J. Odstrcilik, R. Kolar, A. Budai, J. Hornegger, J. Jan, J. Gazarek, T. Kubena, P. Cernosek, O. Svoboda and E. Angelopoulou, "Retinal vessel segmentation by improved matched filtering: evaluation on a new high-resolution fundus image database," *IET Image Processing,* vol. 7, *(4),* pp. 373-383, 2013. Available: http://digital-library.theiet.org/content/journals/10.1049/iet-ipr.2012.0455.

21. S. Holm, G. Russell, V. Nourrit and N. McLoughlin, "DR HAGIS-a fundus image database for the automatic extraction of retinal surface vessels from diabetic patients," *Journal of*

Medical Imaging, vol. 4, *(1),* pp. 014503, 2017. Available: http://www.dx.doi.org/10.1117/1.JMI.4.1.014503.

22. Sunil Kumar Vengalil, Neelam Sinha, Srinivas S S Kruthiventi and R Venkatesh Babu, "Customizing CNNs for blood vessel segmentation from fundus images," in Jan 1, 2016, pp. 1. L. Chen *et al*, "Semantic Image Segmentation with Deep Convolutional Nets and Fully Connected CRFs," 2014. Available: https://arxiv.org/abs/1412.7062.

23. T. Lin, M. Maire, S. Belongie, L. Bourdev, R. Girshick, J. Hays, P. Perona, D. Ramanan, C. L. Zitnick and P. Dollár, "Microsoft COCO: Common Objects in Context," 2014. Available: https://arxiv.org/abs/1405.0312.

24. T. A. Soomro, A. J. Afifi, Junbin Gao, O. Hellwich, M. A. U. Khan, M. Paul and Lihong Zheng, "Boosting sensitivity of a retinal vessel segmentation algorithm with convolutional neural network," in Nov 2017, pp. 1-8.

25. A. Oliveira, S. Pereira and C. A. Silva, "Retinal vessel segmentation based on Fully Convolutional Neural Networks," Expert Systems with Applications, vol. 112, pp. 229-242, 2018. Available: https://www.sciencedirect.com/science/article/pii/S0957417418303816. DOI: 10.1016/j.eswa.2018.06.034.

26. L. Shyam and G. S. Kumar, "Blood vessel segmentation in fundus images and detection of glaucoma," in Jul 2016, pp. 34-38Available: https://ieeexplore.ieee.org/document/7823982

27. E. Deepika and S. Maheswari, "Earlier glaucoma detection using blood vessel segmentation and classification," in Jan 2018, pp. 484-490Available: https://ieeexplore.ieee.org/document/8399120

28. A. O. Joshua, F. V. Nelwamondo and G. Mabuza-Hocquet, "Segmentation of optic cup and disc for diagnosis of glaucoma on retinal fundus images," in Jan 2019, pp. 183-187.

29. W. Ruengkitpinyo, W. Kongprawechnon, T. Kondo, P. Bunnun and H. Kaneko, "Glaucoma screening using rim width based on ISNT rule," in Mar 22, 2015, pp. 1-5Available: https://ieeexplore.ieee.org/document/7110827